Spectrochimica Acta Part A: Molecular and Biomolecular Spectroscopy 131 (2014) 294–302

Contents lists available at ScienceDirect

Spectrochimica Acta Part A: Molecular and Biomolecular Spectroscopy

journal homepage: www.elsevier.com/locate/saa

Synthesis, characterization, antimicrobial activity and carbonic anhydrase enzyme inhibitor effects of salicilaldehyde-*N*-*methyl* *p*-toluenesulfonylhydrazone and its Palladium(II), Cobalt(II) complexes

Saliha Alyar *, Şevki Adem

Department of Chemistry, Science Faculty, Karatekin University, 18100 Çankırı, Turkey

HIGHLIGHTS

- Synthesis of *p*-toluenesulfonicacid-1-methylhydrazide (*ptsmh*).
- Synthesis of salicilaldehyde-*N*-*methyl* *p*-toluenesulfonylhydrazone (*salptsmh*).
- Synthesis of *Co*(*salptsmh*)$_2$ and *Pd*(*salptsmh*)$_2$ complexes.
- Characterization and antimicrobial activities of compounds.
- Carbonic anhydrase enzyme inhibitor effects of compounds.

GRAPHICAL ABSTRACT

Salicilaldehyde-*N*-*methyl* *p*-toluenesulfonylhydrazone (*salptsmh*) derived from *p*-toluenesulfonicacid-1-methylhydrazide (*ptsmh*) and its Pd(II) and Co(II) metal complexes were synthesized for the first time and investigated their antibacterial activities and carbonic anhydrase enzyme inhibitor effects.

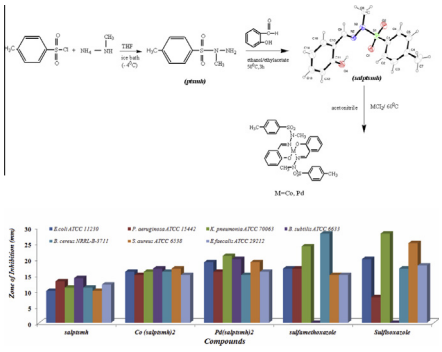

ARTICLE INFO

Article history:
Received 27 March 2014
Received in revised form 12 April 2014
Accepted 22 April 2014
Available online 29 April 2014

Keywords:
Sulfonamides
Pd(II)
Co(II) complexes
Disk diffusion method
CA I
CA II

ABSTRACT

We report the synthesis of the ligand, salicilaldehyde-*N*-*methyl* *p*-toluenesulfonylhydrazone (*salptsmh*) derived from *p*-toluenesulfonicacid-1-methylhydrazide (*ptsmh*) and its Pd(II) and Co(II) metal complexes were synthesized for the first time. The structure of the ligand and their complexes were investigated using elemental analysis, magnetic susceptibility, molar conductance and spectral (IR, NMR and LC-MS) measurements. *Salptsmh* has also been characterized by single crystal X-ray diffraction. ^{1}H and ^{13}C shielding tensors for crystal structure were calculated with GIAO/DFT/B3LYP/6-311++G(d,p) methods in $CDCl_3$. The complexes were found to have general composition [ML_2]. The results of elemental analysis showed 1:2 (metal/ligand) stoichiometry for all the complex. Magnetic and spectral data indicate a square planar geometry for Pd(II) complex and a distorted tetrahedral geometry for Co(II) complexes. The ligand and its metal chelates have been screened for their antimicrobial activities using the disk diffusion method against the selected Gram positive bacteria: *Bacillus subtilis*, *Bacillus cereus*, *Staphylococcus aureus*, *Enterococcus faecalis*, Gram negative bacteria: *Escherichia coli*, *Pseudomonas aeruginosa*, *Klebsiella pneumonia*. The inhibition activities of these compounds on carbonic anhydrase II (CA II) and carbonic anhydrase I (CA I) have been investigated by comparing IC_{50} and Ki values and it has been found that Pd(II) complex have more enzyme inhibition efficiency than *salptsmh* and Co(II) complex.

* Corresponding author. Tel.: +90 5396070947.
E-mail address: saliha@gazi.edu.tr (S. Alyar).

http://dx.doi.org/10.1016/j.saa.2014.04.121
1386-1425/

Introduction

The importance of sulfonamide was realized [1] when sulfonylamide, a key analog of sulfonamide, was reported [2] to be the first antibacterial drug. Sulfonamides were the first effective chemotherapeutic agents employed systematically for the prevention and the cure of bacterial infections in humans and other animal systems [3,4]. Later on, many thousands of molecules containing the sulfanilamide structure have been created since its discovery, yielding improved formulations with greater effectiveness and less toxicity. Sulfa drugs are still widely used for conditions such as acne and urinary tract infections, and are receiving renewed interest for the treatment of infections caused by bacteria resistant to other antibiotics. Also, a number of other activities, some of which have been recently observed, include endotelin antagonism, anti-inflammatory activity, tubular transport inhibition, insulin release, carbonic anhydrase and saluretic action, among others [5].

In order to find better compounds, some metal sulfonamides have attracted much attention due to the fact that complexes showed more activity than both free ligands and the corresponding metallic salts. In particular Ag-sulfadiazine has proved to be an effective topical antimicrobial agent, of significance in burn therapy, better than the free ligand or than $AgNO_3$ [6]. Moreover several Cu(II), Ce(III), Bi(III), Cd(II) and Hg(II) sulfonamide complexes have shown antibacterial activity [7–9]. Specially, a series of copper complexes with heterocyclic sulfonamides was studied and a plausible explanation of their activities was presented [10]. Carbonic anhydrases (CAs, EC 4.2.1.1) form a family of metalloenzymes that play an important function in various physiological and pathological processes [11]. These enzymes are very efficient catalysts for the reversible hydration of carbon dioxide to bicarbonate. Because of the wide distribution of the CAs in many cells, tissues and organs, CAIs are widely used as target enzymes to treat or prevent a multitude of diseases. For this reason, the discovery of new CA inhibitors is very significant [12].

In our previous studies, aliphatic/aromatic bis sulfonamides were synthesized and tested for antimicrobial activity [13–16]. Also, we have reported conformational analysis and c spectroscopic investigation of the methanesulfonic acid hydrazide [17] methanesulfonic acid 1-methylhydrazide [18] some methanesulfonylhydrazone derivatives [19–21]. In this work, Pd(II) and Co(II) complexes of salicilaldehyde-*N*-*methyl*-*p*-toluenesulfonylhydrazone(*salptsmh*) derived from *p*-toluenesulfonicacid-1-methylhydrazide (*ptsmh*) were synthesized and characterized by using elemental analyses, FT-IR, LC-MS spectrometric methods, magnetic susceptibility and conductivity measurements method for the compounds. *Salptsmh* has also been characterized by single crystal X-ray diffraction. ^1H and ^{13}C shielding tensors for crystal structure were calculated with GIAO/DFT/B3LYP/6-311++G(d,p) methods in $CDCl_3$. The antibacterial activities of synthesized compounds were studied against Gram positive bacteria: *B. subtilis* ATCC 6633, *B. cereus* NRRL-B-3711, *S. aureus* ATCC 6538, *E. faecalis* ATCC 29212, Gram negative bacteria: *E. coli* ATCC 11230, *P. aeruginosa* ATCC 15442, *K. pneumonia* ATCC 70063 by using microdilution method (as MICs) and disk diffusion method. The inhibition activities of these compounds on carbonic anhydrase II (CA II) and carbonic anhydrase I (CA I) have been investigated by comparing IC_{50} and Ki values.

Experimental

Physical measurements

The elemental analyses (C, H, N and S) were performed on a LECO CHNS 9320 type elemental analyzer. The IR spectra (4000–400 cm^{-1}) were recorded on a Mattson 1000 FT-IR Spectrophotometer with samples prepared as KBr pellets. LC/MS-APCl was recorded on an AGILENT 1100 Spectrometer. The melting points were measured using an Opti Melt apparatus. TLC was conducted on 0.25 mm silica gel plates (60F 254, Merck). The molar magnetic susceptibilities were measured on powdered samples using Gouy method. The molar conductance measurements were carried out using a Siemens WPA CM 35 conductometer. All solvents were purchased from Merck and reagents were obtained from Aldrich Chem. Co. (ACS grade) and used as received. The experiments were carried out in dynamic nitrogen atmosphere (20 mL min^{-1}) with a heating rate of 10 °C min^{-1} in the temperature range 30–400 °C using platinum crucibles. The microdilution broth method was used to determine the antibacterial activity of compounds against the Gram positive bacteria *B. subtilis* ATCC 6633, *B. cereus* NRRL-B-3711, *S. aureus* ATCC 6538, *E. faecalis* ATCC 29212, Gram negative bacteria: *E. coli* ATCC 11230, *P. aeruginosa* ATCC 15442, *K. pneumonia* ATCC 70063.

Synthesis

General synthesis method of the compounds was depicted schematically in Fig. 1S. (Supporting Information).

Salicilaldehyde-N-methyl p-toluenesulfonylhydrazone (salptsmh)

Ethanol/ethyl acetate (1:1) solution of *p*-toluenesulfonic acid 1-methylhydrazide (1.5 g, 4.72 mmol) was added drop wise to an ethanol/ethyl acetate (1:1) solution of salicilaldehyde (0.52 g, 5.0 mmol), maintaining the temperature at about 323 K. Then, the mixture was stirred for 24 h at room temperature. The precipitated product was crystallized from ethanol/n-hexane (2:1) mixture. The yellow crystalline solid was dried in vacuo and stored at ethanol/n-hexane vapor (2:1). Yield 65%; mp: 155–157 °C. Elemental analysis: Anal. Calcd. For $C_{15}H_{16}SO_3N_2$: C, 60.36; H, 5.70; N, 8.80; S, 10.07. Found: C, 59.80; H, 5.74; N, 9.20; S, 10.22.

Synthesis of Pd(II), Co(II) complexes

All complexes are prepared by the following general method: a sample of anhydrous 0.80 mmol MCl_2, where M: Pd(II) and Co(II), were dissolved in a mixture of methanol and acetonitrile (2/1, 30 mL) and a solution of *salptsmh* (2.0 mmol) in a mixture of acetonitrile (2.0 mL) and NaOH solution in methanol (2.0 mL) was added. The reaction mixture was heated at 60 °C for 1 h. The complexes precipitated quickly after stirring the mixture at room temperature and filtered off, dried in a desiccator over $CaCl_2$.

Pd(*salptsmh*)$_2$ ($C_{30}H_{30}S_2O_6N_4Pd$): Yield 70%; mp: 287–289 °C. Elemental analysis: Calcd. for C, 51.86; H, 4.62; N, 7.56; S, 8.65. Found: C, 50.16; H, 4.45; N, 7.14; S, 8.85.

Co(*salptsmh*)$_2$ ($C_{30}H_{30}S_2O_6N_4Co$): Yield 80%; mp: 284–286 °C. Elemental analysis: Calcd. for C, 55.40; H, 4.94; N, 8.08; S, 9.24. Found: C, 55.31; H, 4.55; N, 8.22; S, 8.95.

Crystallography

For the crystal structure determination, single-crystal of *salptsmh* was used for data collection on a four-circle Rigaku R-AXIS RAPID-S diffractometer (equipped with a two-dimensional area IP detector). Graphite-monochromated Mo Kα radiation (λ = 0.71073 Å) and oscillation scans technique with $\Delta w = 5°$ for one image were used for data collection. The lattice parameters were determined by the least-squares methods on the basis of all reflections with $F^2 > 2\sigma(F^2)$. Integration of the intensities, correction for Lorentz and polarization effects and cell refinement was performed using CrystalClear software [22]. The structures were solved by direct methods using SHELXS-97 [23], and refined by a full-matrix least-squares procedure using the program

SHELXL-97 [23]. H atoms were positioned geometrically and refined using a riding model. The final difference Fourier maps showed no peaks of chemical significance.

Antimicrobial activity

B. subtilis ATCC 6633, *B. cereus* NRRL-B-3711, *S. aureus* ATCC 6538, *E. faecalis* ATCC 29212, *E. coli* ATCC 11230, *P. aeruginosa* ATCC 15442, *K. pneumonia* ATCC 70063 cultures were obtained from Gazi University, Biology Department. Bacterial strains were cultured overnight at 37 °C in Nutrient Broth. During the survey, these stock cultures were stored in the dark at 4 °C.

Disk diffusion method

The synthesize compounds and complexes were dissolved in dimethylsulfoxide (20% DMSO) to a final concentration of 10 mg mL^{-1} and sterilized by filtration by 0.45 μm millipore filters. Antimicrobial tests were then carried out by the disk diffusion method using 100 μL of suspension containing 10^8 CFU mL^{-1} bacteria spread on a nutrient agar (NA) medium. The disks (6 mm in diameter) were impregnated with 20 μL of each compound (200 μg/disk) at the concentration of 10 mg mL^{-1} and placed on the inoculated agar. DMSO impregnated disks were used as negative control. Sulfamethoxazole (300 μg/disk) sulfioxazole (300 μg/disk) were used as positive reference standards to determine the sensitivity of one strain/isolate in each microbial species tested. The inoculated plates were incubated at 37 °C for 24 h for bacterial strains isolates. Antimicrobial activity in the disk diffusion assay was evaluated by measuring the zone of inhibition against the test organisms. Each assay in this experiment was repeated twice [26].

Micro-dilution assays

The minimal inhibition concentration (MIC) values, except one, were also studied for the microorganisms sensitive to at least one of the five compounds determined in the disk diffusion assay. The inocula of microorganisms were prepared from 12 h broth cultures and suspensions were adjusted to 0.5 McFarland standard turbidity. The test compounds dissolved in dimethylsulfoxide (DMSO) were first diluted to the highest concentration (2000 μg mL^{-1}) to be tested, and then serial, twofold dilutions were made in a concentration range from 15.625 to 2000 μg mL^{-1} in 10 mL sterile test tubes containing nutrient broth. The MIC values of each compound against bacterial strains were determined based on a micro-well dilution method [27]. The 96-well plates were prepared by dispensing 95 μL of nutrient broth and 5 μL of the inoculums into each well. One hundred μL from each of the test compounds initially prepared at the concentration of 2400 μg mL^{-1} was added into the first wells. Then, 100 μL from each of their serial dilutions was transferred into eight consecutive wells. The last well containing 195 μL of nutrient broth without compound, and 5 μL of the inoculums on each strip, was used as negative control. The final volume in each well was 200 μL. The contents of the wells were mixed and the micro-plates were incubated at 37 °C for 24 h. All compounds tested in this study were screened twice against each microorganism. The MIC was defined as the lowest concentration of the compounds to inhibit the growth of microorganisms.

Enzyme assay and inhibition studies

Carbonic anhydrase activity was measured using esterase and hydratase methods as described earlier [28,29]. To determine the inhibitory potency of effects of compounds on hCA I and hCA II, five different concentrations of compounds were added to the reaction mixture and the enzyme activity was measured. All compounds were examined in triplicate at each concentration used. The IC_{50} values as the inhibitor concentration that causes a 50% decline in enzyme activity under comparable assay and laboratory conditions were calculated from inhibitor dose response curves. On esterase activity, the Ki constants were calculated using the Cheng–Prusoff equation.

Theoretical calculations

The molecular geometry optimizations and vibration frequency calculations were performed with the Gaussian 03W software package by using DFT approaches in addition to the determination of crystal structure [24]. The split valence 6-311++G(d,p) basis set was used for the expansion of the molecular orbital [25]. The geometries were fully optimized without any constraint with the help of an analytical gradient procedure implemented within the Gaussian 03W program. All the parameters were allowed to relax and all the calculations converged to an optimized geometry which corresponds to a true energy minimum as revealed by the lack of imaginary values in the wave number calculations. The ^1H and ^{13}C NMR chemical shifts of the compounds were calculated in $CDCl_3$ using the GIAO method. The energy gap of HOMO–LUMO explains the prospective charge transfer interaction within the molecule, and in this study, the frontier orbital energy gap has obtained at B3LYP method using LanL2DZ basis set.

Results and discussion

Crystal structure analysis

Molecular structure with the atom-numbering scheme of *salptsmsh* was given in Fig. 1(a). Crystal data and structure refinement parameters of *salptsmsh* were given in Table 1. Experimental geometric parameters are given in Table 2. The crystal structure contains intramolecular hydrogen bonds which play an important role in stabilization, O4—H4···N2 = 2.588(5) Å, <(N3—H3···$O3^i$) = 145.7°. The presence of an O4—H4···N2 intramolecular hydrogen bond has been found to be a general feature in the molecular structures of sulfonylhydrazones, thiocarbazides and thiocarbazones [30–33]. Thus, the length of the C—O bond is 1.364 Å which is consistent with a single bond; while the C=N bond distance is 1.279 Å. The geometry around S1 atom is significantly deviated from that of regular tetrahedral, The maximum and minimum angles around S1 are 120.7(3)° and 105.6(2)°, respectively. In all essential details, the geometry of the molecule regarding bond lengths and angles of the compound are in good agreement with the values observed in similar structures [20,34]. Unit cell content indicating the crystal structure of the molecule is given in Fig. 1(b).

FT-IR spectra

IR spectra support the structure of the complexes by the determination of the coordination modes. The changes in the characteristic vibrations of the ligands were compared with complexes. The important IR spectral bands of the compounds along with their tentative assignments are given in Table 3. In the IR spectrum of the *ptsmh*, strong bands observed at 3345, 3261 and 1640 cm^{-1} are assigned to the $\upsilon_{as}(NH_2)$, $\upsilon_s(NH_2)$ and $\delta(NH_2)$ modes, respectively. Shifting of the ν(C=N) frequency at 1620 cm^{-1} of the *salptsmh* to a lower frequency by ~18–24 cm^{-1} (1596–1602 cm^{-1}) in all of its metal complexes (Table 3) is the evidence of the nitrogen bonding of the (C=N) group to the central metal atom. Shifting of the (C—O) stretching frequency at 1244 cm^{-1} to a higher frequency by ~36–51 cm^{-1} (1280–1295 cm^{-1}) in the complexes is also evidence of the oxygen bonding of the (C—O) group to the metal atom. This is further confirmed by the appearance of the new band at 555–570 cm^{-1} due to (M—O) stretching modes in the metal

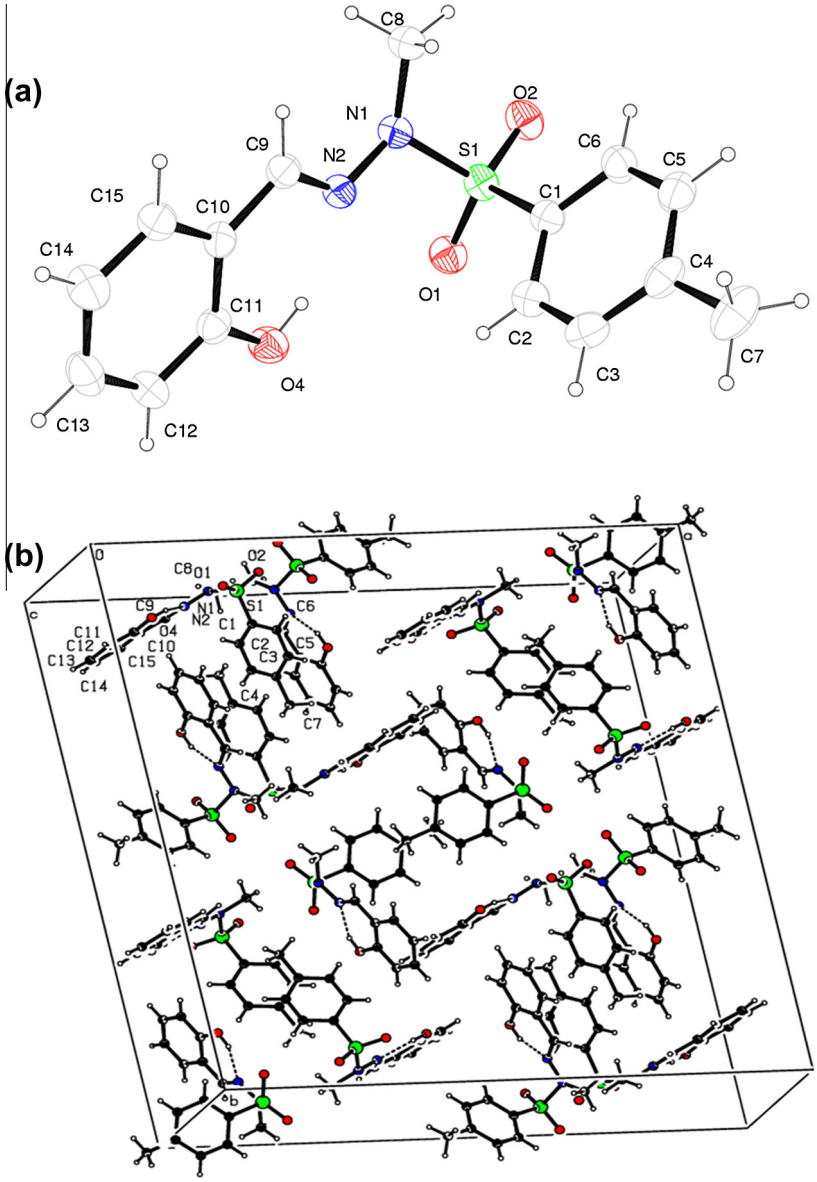

Fig. 1. The molecular structure of *salptsmh* with the atom-numbering scheme; displacement ellipsoids are drawn at the 50% probability level (a) and the crystal packing (b) of *salptsmh*.

complexes. In the IR spectra of *salptsmh*, vibrational band observed at 1144 cm^{-1} and 1333 cm^{-1} are assigned to asymmetric and symmetric SO_2 stretching modes, respectively. Not shifting of symmetric and asymmetric SO_2 modes in the complexes is attributed to not participating in coordination.

NMR spectra

The NMR spectra (^1H, ^{13}C) of *ptsmh* and *salptsmh* were measured and interpreted in $CDCl_3$. In order to facilitate the interpretation of the NMR spectra, quantum-chemical calculations were performed using B3LYP/6-311G++(d,p) basis set *salptsmh* in $CDCl_3$ phase. Isotropic shielding tensors of ^{13}C and ^1H were changed into chemical shifts by using a linear relationship suggested by Ünal et al. [35]. The experimental and calculated chemical shift values are shown in Table 4. The ^{13}C NMR and ^1H NMR spectrum of the *salptsmh* in chloroform are given in Fig. 2. ^1H NMR spectrum of *ptsmh*, C**H**$_3$—Ar and N—C**H**$_3$ proton signals gave the following results: 2.263 ppm and 3.419 ppm respectively. The N**H**$_2$ proton shifts displayed as singlet at 4.6 ppm. In Table 4, the ^1H NMR spectrum of *salptsmh*, C**H**$_3$—Ar and N—C**H**$_3$ protons appeared at 2.425 ppm and 3.214 ppm were calculated at 2.354 ppm and 3.160 ppm. A signal was also observed at δ = 10.816 ppm of the phenolic **H**—O— group and calculated at 5.101 ppm. The singlet peak belonging to the azomethine C**H**=N proton at 8.749 ppm (calculated 7.26 ppm) indicates the predominance of the phenolic-imine tautomer in the *salptsmh* [20,36]. The ^{13}C NMR spectrum of ptsmh, CH_3—Ar and N—CH_3 carbon signals gave the following results: 20.390 ppm and 33.476 ppm respectively. The ^{13}C NMR spectra of *salptsmh* were assigned at δ 21.616 ppm, 33.590 ppm (calculated 21.025 ppm, 29.477 ppm respectively) for C**H**$_3$—Ar and N—C**H**$_3$ groups. Azomethine C**H**=N carbon peak at 144.782 ppm (calculated 137.245 ppm) indicates the predominance for *salptsmh*. Signals in the δ 117.208–158.136 ppm region belong to aromatic Ar—**C**-atoms.

Mass spectra

Fragmentation steps of all compounds in LC-MS spectra are exhibitited in Figs. S2 and S3 (Supporting Information). The

Table 1
Crystal data and structure refinement for *salptsmh*.

Empirical formula	$C_{15}H_{16}N_2O_3S$
Formula weight	304.37
Temperature	293(2) K
Wavelength	0.71073 Å
Crystal system	Tetragonal
Space group	$I\,41/a$
Unit cell dimensions	a = 28.9612(2) Å α = 90°
	b = 28.9612(2) Å β = 90°
	c = 7.2364(1) Å γ = 90°
Volume	6069.54(12) Å^3
Z	16
Density (calculated)	1.332 g/cm^3
Absorption coefficient	0.224 mm^{-1}
$F(000)$	2560
Crystal	Needle; yellow
Crystal size	0.20 × 0.02 × 0.02 mm^3
θ Range for data collection	2.8–26.4°
Index ranges	$-36 \leqslant h \leqslant 36$, $-36 \leqslant k \leqslant 36$, $-9 \leqslant l \leqslant 7$
Reflections collected	20,324
Independent reflections	1321[R_{int} = 0.1166]
Completeness to θ = 26.4°	99.4%
Max. and min. transmission	0.948 and 0.978
Refinement method	Full-matrix least-squares on F^2
Data/restraints/parameters	1321/0/193
Goodness-of-fit on F^2	0.989
Final R indices [$F^2 > 2\sigma(F^2)$]	R_1 = 0.076, wR_2 = 0.167
R indices (all data)	R_1 = 0.180, wR_2 = 0.220
Extinction coefficient	0.00
Largest diff. peak and hole	0.243 and −0.234 e Å^{-3}

Table 2
Selected bond distances (Å) and angles (°) for *salptsmh*.

The bond lengths (Å)	
S(1)—O(2) 1.421(4)	S(1)—O(1) 1.427(4)
S(1)—C(1) 1.748(5)	S(1)—N(1) 1.680(4)
N(2)—N(1) 1.374(6)	N(2)—C(9) 1.278(7)
C(2)—H(2) 0.930(5)	C(2)—C(1) 1.372(7)
C(2)—C(3) 1.385(8)	C(1)—C(6) 1.384(7)
C(12)—H(12) 0.930(6)	C(12)—C(11) 1.372(7)
C(12)—C(13) 1.390(9)	N(1)—C(8) 1.467(7)
C(11)—O(4) 1.364(6)	
The bond angles (°)	
O(2)—S(1)—O(1) 120.7(3)	O(2)—S(1)—C(1) 109.4(3)
O(2)—S(1)—N(1) 105.6(2)	O(1)—S(1)—C(1) 108.5(3)
O(1)—S(1)—N(1) 105.9(2)	C(1)—S(1)—N(1) 105.7(2)
N(1)—N(2)—C(9) 122.6(4)	N(2)—N(1)—C(8) 120.2(4)
C(1)—C(2)—C(3) 119.7(5)	S(1)—C(1)—C(2) 119.9(4)
S(1)—C(1)—C(6) 120.1(4)	

Table 3
Major IR absorption bands (cm^{-1}) of the compounds.

Assignment	*Ptsmh*	*Salptsmh*	*Co(salptsmh)*$_2$	*Pd(salptsmh)*$_2$
υ(C—H)$_{ar}$	3040	3045	2940	2935
υ(C=N)	–	1620	1602	1596
υ(C=C)	–	1575	1572	1570
υ_{as}(SO_2)	1330	1333	1331	1329
υ(C—O)	–	1244	1295	1280
υ_s(SO_2)	1140	1144	1148	1142
υ(M—O)	–	–	555	570

salptsmh gives the following fragmentation peaks: 304.8(15.5%) as molecular ion peak by losing of one proton, 289.9(18.9%) which occurs by losing of methyl group, 198.6 (100%) belongs to *ptsmh* ($C_8H_{12}SO_2N_2$). *Pd*(*salptsmh*)$_2$ gives the following peaks: 711.8 (8.9%) and 605.8 (20.5%) which occurs by losing of *Pd* atom and fragment III is observed 303.1 (100%) from the removal of the two (phen+ −M) groups. *Co*(*salptsmh*)$_2$ gives the following peaks: 664.90 (12.6%) and 604.9 (27.1%) which occurs by losing of Co atom and fragment III is observed 303.5 (56%) from the removal of the two (phen+ −M) groups.

Table 4
The experimental and theoretical ^{1}H and ^{13}C NMR chemical shifts δ (ppm) for *salptsmh*.

Assignment	δ (exp.)	B3LYP/6-311++G(d,p)[a] δ (calc.)
C-1	132.267	138.925
C-2	131.206	128.789
C-3	131.842	129.079
C-4	149.211	146.652
C-5	131.842	128.800
C-6	131.206	128.789
C-7(CH_3)	21.616	21.025
C-8(CH_3—N)	33.590	29.477
C-9(C=N)	144.782	137.245
C-10	119.439	122.321
C-11	158.136	155.32
C-12	117.548	115.569
C-13	128.035	129.823
C-14	117.208	119.789
C-15	129.958	133.967
H-2	7.762	8.387
H-3	7.219	7.218
H-5	7.215	7.460
H-6	7.742	7.747
H-7(CH_3)	2.425	2.356
H-8(CH_3—N)	3.214	3.160
H-9(CH=N)	8.749	7.26
H-12	6.926	6.751
H-13	7.285	7.201
H-14	6.908	6.895
H-15	7.291	7.212
OH	10.816	5.101

[a] σ Transform into δ using equations given in Ref. [35]; $\delta^{13}C = 175.7–0.963\ \sigma^{13}C$ and $\delta^{1}H = 31.0–0.970\ \sigma^{1}H$.

Electronic spectra and magnetic behavior

The reaction of Schiff base with transition metal ions in 1:2 M ratio lead to the formation of Schiff base sulfonamides complexes of the types, [ML_2] (M = Co(II), Pd(II)) (Fig. S1) (Supporting Information). The molar conductivities (Λ_m) of 10^{-3} M solutions of the complexes were measured in DMSO at room temperature. Conductivity results show that complexes are non-electrolyte. The significant electronic spectra of the ligand and complexes were recorded in DMSO. The important bands of the ligands and the complexes were observed in the region of 293–260 and 430–332 nm. The magnetic moments of the complexes (as B.M.) were measured at room temperature. The electronic spectrum of the Pd(II) complex 353–354 nm, attributed to the $^1A_{2g} \rightarrow {}^1B_{1g}$ and $^3B_{1g} \rightarrow {}^1A_{1g}$ transitions respectively, indicated a square planar environment around the metal ion. The observed magnetic moments of the Palladium(II) complex were 0 B.M. The magnetic moment value (3.89 B.M.) for Co(II) complex, the broad band in its electronic spectrum centered at 425 nm, suggested a tetrahedral geometry around the Co(II) ion. Also, the $^4T_{1(F)} \rightarrow {}^4A_2$ transition observed in the tetrahedral geometry [37].

Frontier molecular orbital analysis

The calculations indicate that the ligand and complex compounds have 80 and 158 occupied molecular orbital, respectively. The energy band gaps between the highest occupied molecular orbital (HOMO) and the lowest unoccupied molecular orbital (LUMO) energies for mentioned compounds, have been calculated and is given in Fig. S4. The frontier molecular orbitals play an important role in the electronic and optical properties, as well as

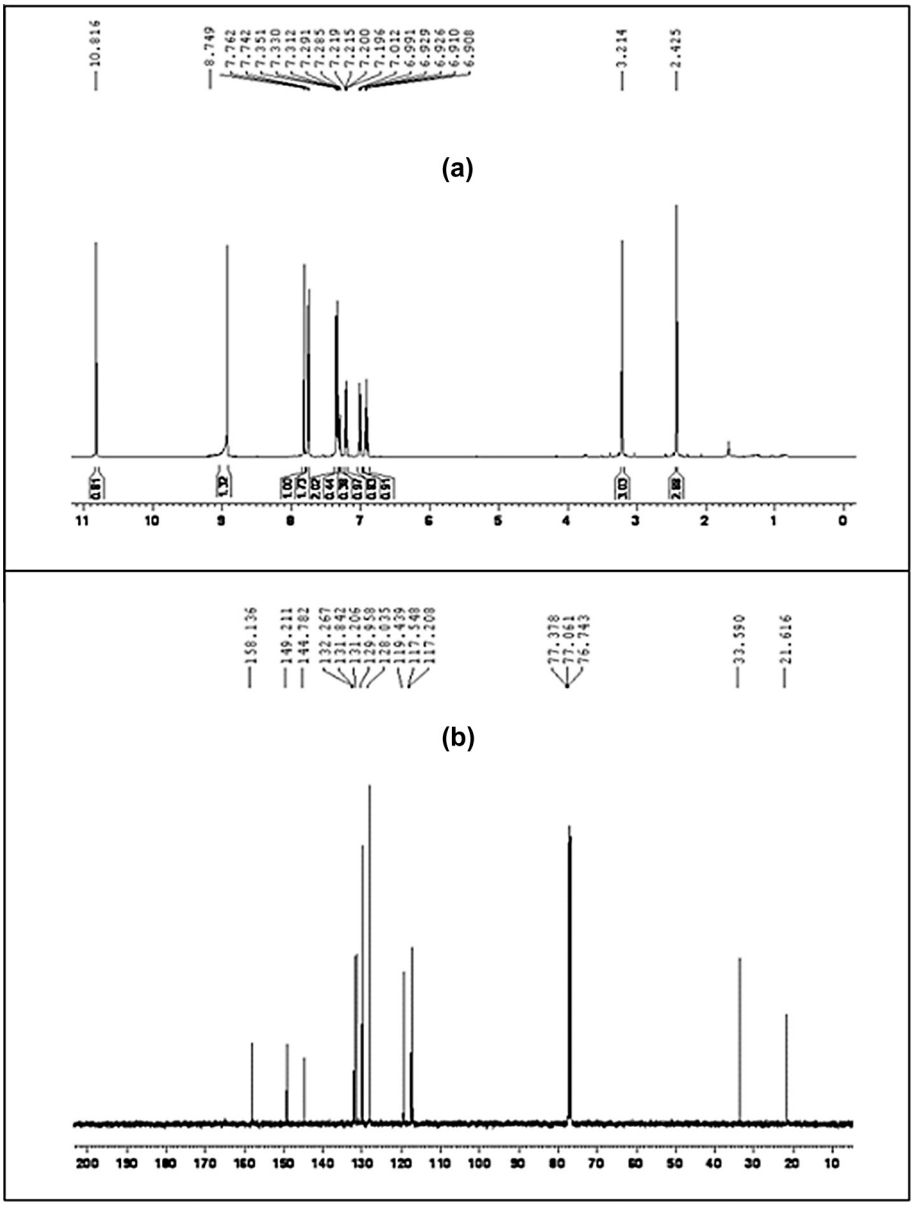

Fig. 2. (a) ^{1}H NMR spectrum of the *salptsmh*, (b) ^{13}C NMR spectrum of the *salptsmh*.

in UV–vis spectra and chemical reactions [38]. Also, the energy band gap between HOMO and LUMO is a critical parameter in determining molecular electrical transport properties and electronic systems with a larger HOMO–LUMO gap should be less reactive than those with a smaller gap [39]. The energy band gap of HOMO–LUMO explains the prospective charge transfer interaction within the molecule, and in this study, the frontier orbital energy band gap in case of ligand compound is found to be 4.18 eV obtained at B3LYP method using LanL2DZ basis set. Also, the frontier orbital energy gap in case of Co(II) and Pd(II) complex was found to be 2.54 and 2.14 eV obtained at B3LYP method using LanL2DZ basis set, respectively. The case of complex energy band gap is reduced by about 40–50%.

The LUMO energy is very important descriptors which describe electrophilicity of the compound and its level has the importance because of the donor–acceptor interactions. Molecules with lower LUMO energy values accept the electrons more easily than higher's. The lower LUMO energy and larger $\Delta E_{(\mathrm{HOMO-LUMO})}$ band gap affect the binding affinities to the biologic molecules, therefore LUMO energy and $\Delta E_{(\mathrm{HOMO-LUMO})}$ band gap are important factors for activities of sulfonamide compounds.

The biological activity is reverse relationship to the $\Delta E_{(\mathrm{HOMO-LUMO})}$ band gap. The biological activity and Carbonic anhydrase activity of the studied compounds increase with the lower $\Delta E_{(\mathrm{HOMO-LUMO})}$ band gap. Respective values of $\Delta E_{(\mathrm{HOMO-LUMO})}$ band gap and biological activity are in following orders. For $\Delta E_{(\mathrm{HOMO-LUMO})}$ band gap: *salptsmh* > Co(*salptsmh*)$_2$ > *Pd*(*salptsmh*)$_2$ and for biological activity and Carbonic anhydrase activity: *salptsmh* < Co(*salptsmh*)$_2$ < *Pd*(*salptsmh*)$_2$.

Biological activity

The test compounds were screened in vitro for their antibacterial activity against three Gram-positive species (*B. subtilis*, *S. aureus*, *E. faecalis*) and three Gram-negative species (*E. coli*, *P. aeruginosa*, *K. pneumonia*) of bacterial strains by the microdilution and disk diffusion methods (Tables 5 and 6). The results were compared with those of the standard drugs sulfamethoxazole

Table 5
The MICs of antibacterial activity of the compounds.

Bacteria strains	MIC μg/mL (mM)				
	Salptsmh	*Co(salptsmh)*$_2$	*Pd(salptsmh)*$_2$	Sulfamethoxazole	Sulfisoxazole
Gram-negative					
Eschericha coli ATCC 11230	500 (1.64)	125 (0.187)	62.5 (0.087)	64 (0.25)	23.4 (0.088)
Pseudomonas aeruginosa ATCC 15442	500 (1.64)	125 (0.187)	125 (0.175)	64 (0.25)	375 (1.40)
Klebsiella pneumonia ATCC 70063	250 (0.82)	125 (0.187)	62.5 (0.087)	16 (0.063)	23.4 (0.088)
Gram-positive					
Bacillus subtilis ATCC 6633	250 (0.82)	62.5 (0.094)	62.5 (0.087)	1500 (5.92)	–
Bacillus cereus NRRL-B-3711	500 (1.64)	62.5 (0.094)	250 (0.350)	16 (0.063)	375 (0.088)
Staphylococcus aureus ATCC 6538	500 (1.64)	125 (0.187)	62.5 (0.087)	32 (0.126)	93.75 (0.35)
Enterococcus faecalis ATCC 29212	250 (0.82)	250 (0.0374)	250 (0.350)	32 (0.126)	93.75 (0.35)

Table 6
Measured inhibition zone diameter (mm) of the compounds and antibiotics by disk diffusion method.

Bacteria strains	*Diameter inhibition zone* [a](mm.200 μg/disk)				
	Salptsmh	*Co(salptsmh)*$_2$	*Pd(salptsmh)*$_2$	Sulfamethoxazole	Sulfisoxazole
Gram-negative					
Eschericha coli ATCC 11230	10	16	19	17	20
Pseudomonas aeruginosa ATCC 15442	13	15	16	17	8
Klebsiella pneumonia ATCC 70063	11	16	21	24	28
Gram-positive					
Bacillus subtilis ATCC 6633	14	17	20	–	–
Bacillus cereus NRRL-B-3711	11	16	15	28	17
Staphylococcus aureus ATCC 6538	10	15	19	15	25
Enterococcus faecalis ATCC 29212	12	12	16	15	18

<10: weak; >10: moderate; >16: significant.
[a] Average values.

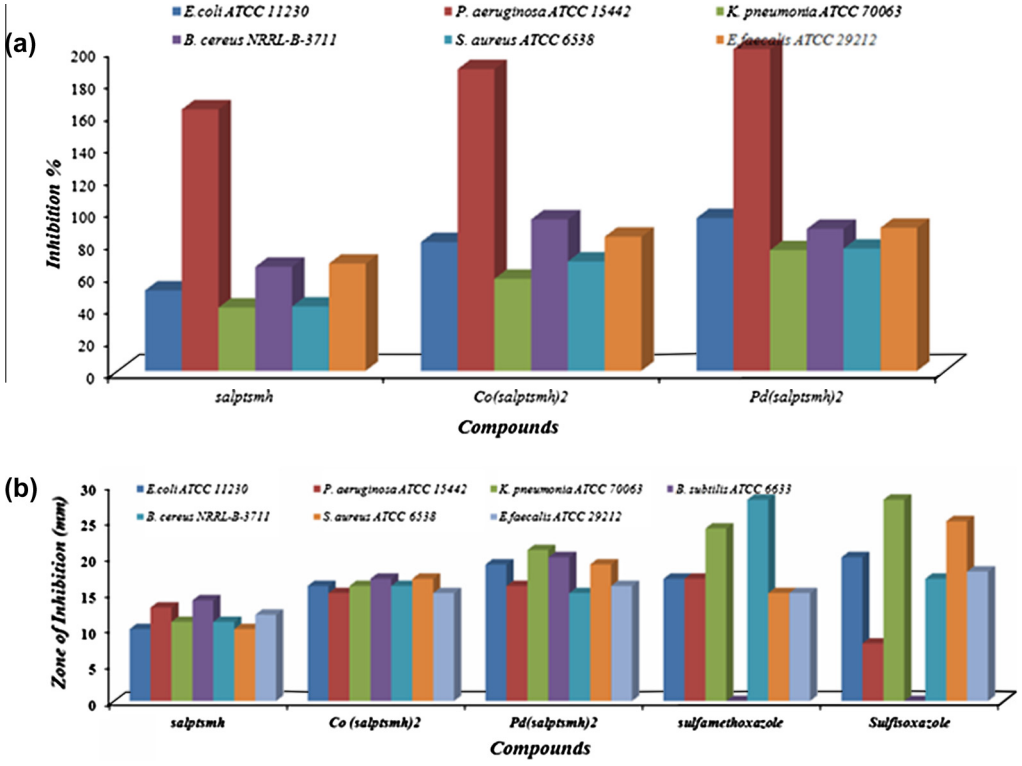

Fig. 3. (a) Comparison of antibacterial activite (MIC) and (b) Comparison of antibacterial activite (disk).

Table 7
Inhibitor effects of compounds for the esterase and hydratase activities of human CA-I and II.

Compounds	hCA I			hCA II		
	Esterase activity		Hydratase activity	Esterase activity		Hydratase activity
	IC_{50} (μM)	Ki (μM)	IC_{50} (μM)	IC_{50} (μM)	Ki (μM)	IC_{50} (μM)
Salptsmh	431 ± 22 (32–164)	280	Uneffect	113 ± 3.8 (32–164)	0.200	74 ± 3
Pd(*salptsmh*)$_2$	69 ± 1.2 (15–90)	2.32	9.6 ± 0.03	25 ± 1.4 (7–38)	0.044	1.5 ± 0.6
Co(*salptsmh*)$_2$	402 ± 26 (179–539)	13.49	82.6 ± 0.03	130 ± 14 (85–426)	0.230	13 ± 0.1
Acetazolamide	0.360 ± 0.05 (0.072–0.72)	0.240	0.108 ± 0.02 (0.042–0.21)	0.015 ± 0.003 (0.0036–0.036)	2.8×10^{-5}	0.0053 ± 0.0009 (0.0021–0.01)

and sulfioxazole (Fig. 3). As the disk diffusion assay results evidently show that *Pd*(*salptsmh*)$_2$ has exhibited the strong inhibition effect against most of test bacteria whereas *salptsmh* has weaker activity. Similar results were also reported by Özmen et al. [40].

The ligand and its complexes show the highest activities against *B. subtilis* which is the mostly effected by *Pd*(*salptsmh*)$_2$ having the diameter zone of 20 mm. All compounds have moderate activity against *P. aeruginosa* at in the diameter zone of 13–16 mm whereas sulfisoxazole, the drug used as standard, has been found less active (8 mm) against the bacteria mentioned above. According to the MIC's results shown in Table 5 the compounds possess a broad spectrum of activity against the tested bacteria at the concentrations of 62.5–500 μg/mL [41]. The *Pd*(*salptsmh*)$_2$ *and Co*(*salptsmh*)$_2$ have shown activity against *P. aeruginosa* and *B. cereus* at a concentration of 62.5 μg/mL; 125 μg/mL whereas sulfisoxazole, the drug used as standard, has been found less active against the bacteria. Also, the antimicrobial activity is highly influenced by the nature of the *salptsmh* and its complexes the order of the activity in mM for all test bacteria is as follows (Table 5).

Percentage of inhibition for the compounds exhibited in Fig. 3(a) that was expressed as excellent activity (120–200% inhibition), good activity (90–100% inhibition), moderate activity (75–85% inhibition), significant activity (50–60% inhibition), negligible activity (20–30% inhibition) and no activity [42]. As seen in Fig. 3, all compounds have excellent activity against *P. aeruginosa.* *Pd*(*salptsmh*)$_2$ shows good activity while *Co*(*salptsmh*)$_2$ has moderate activity against *E. coli.*

Carbonic anhydrase activity results

Sulfonamides compose an important class of carbonic anhydrase inhibitors. Some compounds such as sulfapyridine, sulfadiazine and acetazolamide are used as medicaments. Therefore, different sulfonamide derivatives have been synthesized and investigated for their inhibition activity on the carbonic anhydrase isoenzymes. These new compounds were tested to determine their inhibitory effects on the hydratase and esterase activities of cytosolic CA isozymes. Table 7 depicted the in vitro effects of compounds on esterase and hydratase activities of hCAI and hCAII. Compounds showed different inhibitory effect on the esterase and hydratase activity of enzymes.

For esterase activity, the compound *Pd*(*salptsmh*)$_2$ behave as potent inhibitors against hCA I and hCA II with IC_{50} value 69 and 25 μM, respectively, whereas compound *Co*(*salptsmh*)$_2$ and *salptsmh* showed poor inhibitory activity when compared to *Pd*(*salptsmh*)$_2$. Effect of the *Pd*(*salptsmh*)$_2$ at different concentrations on esterase and hydratase activity of hCA-I and hCA-II given in Fig. S5. Compounds *Co*(*salptsmh*)$_2$ and *salptsmh* exhibit the same potency as hCA II inhibitors, with IC_{50} values in the range of 113–130 μM. Same derivatives demonstrated almost similar inhibitor effect on hCA I, with IC_{50} values in range 402–431 μM.

For hydratase activity; against the cytosolic isozymes hCA I and hCA II, *Pd*(*salptsmh*)$_2$ showed a strong inhibitory effect, with IC_{50} values 9.6 and 1.5 μM, respectively. Isoforms hCA I and II were moderately inhibited by *Co*(*salptsmh*)$_2$. Synthesized sulfonamide showed weak inhibitory effect on most abundant and rapid isoform hCA II, whereas this derivative did not show any inhibitor effect on isoform hCA I. The new compounds showed weak hCA I and II inhibitory efficiency as compared to the clinically used acetazolamide. These data clearly inform that palladium may be enhanced the activity of the sulfonamides complexes.

Conclusions

In this study we have reported the synthesis of *salptsmh* and its Co(II) and Pd (II) complexes. The structural characterizations of the synthesized compounds were made by using the elemental analyses, spectroscopic methods, magnetic and conductance studies. The biological activity screening showed that complexes have more activity than ligands against the tested bacteria. All compounds have excellent activity against *P. aeruginosa.* *Pd*(*salptsmh*)$_2$ shows good activity while *Co*(*salptsmh*)$_2$ has moderate activity against *E. coli.* *Co*(*salptsmh*)$_2$ and *salptsmh* showed poor inhibitory activity when compared to *Pd*(*salptsmh*)$_2$ against CA II. Although the case of complex the $\Delta E_{(HOMO-LUMO}$ energy band gap is reduced by about 40–50%, the biological activity and Carbonic anhydrase activity of the studied compounds increased in a manner inversely proportional.

Acknowledgments

The authors would like to thank Karatekin University BAP (Grant No: 05/2011-05) for the financial support of this project. We would like to thank also to Dr. Ertan Şahin for XRD measurement.

Appendix A. Supplementary material

Crystallographic data that were deposited in CSD under CCDC registration number 894662 contain the supplementary crystallographic data for this Letter. These data can be obtained free of charge from the Cambridge Crystallographic Data Centre (CCDC) via www.ccdc.cam.ac.uk/data_request/cif and are available free of charge upon request to CCDC, 12 Union Road, Cambridge, UK (fax: +44 1223 336033, e-mail: deposit@ccdc.cam.ac.uk). Supplementary data associated with this article can be found, in the online version, at http://dx.doi.org/10.1016/j.saa.2014.04.121.

References

[1] G. Domagk, Deut. Med. Wochenschr. 61 (1935) 250–258.
[2] G.L. Mandell, W.A. Petri, J.G. Hardman, L.E. Limbird, P.B. Molinoff, R.W. Ruddon, A.G. Gilman, Goodman's and Gilman's the Pharmacological Basis of Therapeutics, ninth ed., McGraw-Hill, New York, 1996. pp. 1073–1101.
[3] X. He, L. Tang, L. He, P. Xu, Huaxi Yike Daxue Xuebao 19 (1988) 317–322.
[4] T. Nogrady, Medicinal Chemistry, second ed., Oxford University Press, New York, 1988. p. 383.
[5] M.E. Wolff, Burger's Medicinal Chemistry and Drug Discovery, vol. 2, fifth ed., Wiley, Laguna Beach, 1996, pp. 528–576.

[6] J.E.F. Reynolds, The Extra Pharmacopoeia, Royal Pharmaceutical Society, London, 1996. pp. 580–581.
[7] A. Bult, in: H. Siegel, Metal Ions in Biological Systems, M. Dekker, Chapter 16, New York, 1983, pp. 261–277.
[8] G. Casanova, G. Alzuet, J. Borrás, J. Timoneda, S. García-Granda, I. Cándano González, J. Inorg. Biochem. 56 (1994) 65–76.
[9] Z.H. Chohan, K. Mahmood-Ul-Hassan, M. Khan, C.T. Supuran, J. Enzym. Inhib. Med. Chem. 20 (2005) 183–188.
[10] E. Kremer, G. Facchin, P. Estévez E, E.J. Alborés, Baran, J. Ellena, M.H. Torre, J. Inorg. Biochem. 100 (2006) 1167–1175.
[11] K.M. Gilmour, Comp. Biochem. Physiol. – A Mol. Integr. Physiol. 157 (3) (2010) 193–197.
[12] C.T. Supuran, Nat. Rev. Drug. Discov. 7 (2008) 168–181.
[13] S. Alyar, N. Karacan, J. Enzym. Inhib. Med. Chem. 24 (2009) 986–992.
[14] N. Özbek, H. Katırcıoglu, N. Karacan, T. Baykal, Bioorg. Med. Chem. 15 (2007) 5105–5109.
[15] S. Alyar, N. Ozbek, N. Karacan, Drug. Future 32 (2007) 126–127.
[16] N. Özbek, S. Alyar, N. Karacan, Drug. Future 32 (2007) 127–128.
[17] A. Ienco, C. Mealli, P. Paoli, N. Dodoff, Z. Kantarci, N. Karacan, New J. Chem. 23 (1999) 1253–1260.
[18] N. Özbek, S. Alyar, N. Karacan, J. Mol. Struct. 938 (2009) 48–53.
[19] N.I. Dodoff, U. Ozdemir, N. Karacan, M.C. Georgieva, S.M. Konstantinov, M.E. Stefanova, Z. Naturforsch. 54b (1999) 1553–1562.
[20] N. Özbek, G. Kavak, Y. Özcan, S. Ide, N. Karacan, J. Mol. Struct. 919 (2009) 154–159.
[21] S. Alyar, Ü.Ö. Özmen, N. Karacan, O.S. Senturk, K.A. Udachin, J. Mol. Struct. 889 (2008) 144–149.
[22] Rigaku/MSC Inc: 9009 new Trails Drive, The Woodlands, TX 77381, 2005.
[23] G.M. Sheldrick, SHELXS97 and SHELXL97, University of Göttingen, Germany, 1997.
[24] M.J. Frisch, G.W. Trucks, H.B. Schlegel, G.E. Scuseria, M.A. Robb, J.R. Cheeseman, J.A. Montgomery Jr., T. Vreven, K.N. Kudin, J.C. Burant, J.M. Millam, S.S. Iyengar, J. Tomasi, V. Barone, B. Mennucci, M. Cossi, G. Scalmani, N. Rega, G.A. Petersson, H. Nakatsuji, M. Hada, M. Ehara, K. Toyota, R. Fukuda, J. Hasegawa, M. Ishida, T. Nakajima, Y. Honda, O. Kitao, H. Nakai, M. Klene, X. Li, J.E. Knox, H.P. Hratchian, J.B. Cross, C. Adamo, J. Jaramillo, R. Gomperts, R.E. Stratmann, O. Yazyev, A.J. Austin, R. Cammi, C. Pomelli, J.W. Ochterski, P.Y. Ayala, K. Morokuma, G.A. Voth, P. Salvador, J.J. Dannenberg, V.G. Zakrzewski, S. Dapprich, A.D. Daniels, M.C. Strain, O. Farkas, D.K. Malick, A.D. Rabuck, K. Raghavachari, J.B. Foresman, J.V. Ortiz, Q. Cui, A.G. Baboul, S. Clifford, J. Cioslowski, B.B. Stefanov, G. Liu, A. Liashenko, P. Piskorz, I. Komaromi, R.L. Martin, D.J. Fox, T. Keith, M.A. Al-Laham, C.Y. Peng, A. Nanayakkara, M. Challacombe, P.M.W. Gill, B. Johnson, W. Chen, M. W. Wong, C. Gonzalez, J.A. Pople Gaussian 03: Revision B.04 Gaussian, Inc., Pittsburgh, PA, 2003.
[25] P.C. Hariharan, J.A. Pople, J. Chem. Phys. 27 (1974) 209–214.
[26] A.W. Bauer, W.M. Kirby, J.C. Sherris, M. Turck, Am. J. Clin. Pathol. 45 (1966) 493–496.
[27] G. Küçükgüzel, A. Kocatepe, E.D. Clercq, F. Şahin, M. Güllüce, Eur. J. Med. Chem. 41 (2006) 353–359.
[28] J.A. Verpoorte, S. Mehta, J.T. Edsall, J. Biol. Chem. 242 (1967) 4221–4229.
[29] K.M. Wilbur, N.G. Anderson, J. Biol. Chem. 176 (1948) 147–154.
[30] M. Soriano-Garcia, J. Valdes-Martinez, R.A. Toscano, Acta Crystallogr. C 44 (1988) 1247–1249.
[31] S. Ito, A. Kakehi, K. Okada, Heterocycles 51 (1999) 2949–2960.
[32] D. Chattppadhyay, S.K. Mazumdar, T. Banerjee, S. Ghosh, T.C.W. Mak, Acta Crystallogr. C 44 (1988) 1025–1028.
[33] S.W. Ng, Z. Kristallogr, New Cryst. Struct. 212 (1997) 277–278.
[34] T. Hokelek, S. Bilge, S. Demiriz, B. Özgüç, Z. Kılıç, Acta Cryst. C. 60 (2004) 803–805.
[35] A. Ünal, B. Eren, Spectrochim. Acta Part A Mol. Biomol. Spectrosc. 114 (2013) 129–136.
[36] N. Ancın, O. Celik, S.G. Öztas, S. Ide, Struct. Chem. 18 (2007) 347–352.
[37] A.B.P. Lever, Inorganic Electronic Spectroscopy, second ed., Elsevier, Amsterdam, 1984. p. 534.
[38] Ç. Yüksektepe, H. Saraçoğlu, N. Çalışkan, İ. Yilmaz, A. Cukurovali, Bull. Korean Chem. Soc. 31 (2010) 3553–3560.
[39] V. Arjunan, P.S. Balamourougane, C.V. Mythili, S. Mohan, J. Mol. Struct. 1003 (2011) 92–102.
[40] Ü.Ö. Özmen, N. Akkaya, N. Özbek, Inorg. Chim. Acta 400 (2013) 13–19.
[41] Z.H. Chohan, A.U. Shaıkh, M.M. Nasee, C.T. Supuran, J. Enzyme Inhib. Med. Chem. 21 (2006) 771–781.
[42] N. Sultana, A. Naz, M.S. Arayne, M.A. Mesaik, Synthesis, J. Mol. Struct. 969 (2010) 17–24.